Effects of tampering on rare-gas core-shell clusters irradiated by resonantly tuned soft-x-ray pulses

Rishi Pandit, Valerie Becker, Jeremy Thurston, Kasey Barrington, Zachary Hartwick, Nicolas Bigaouette, Lora Ramunno, and Edward Ackad

Phys. Rev. A **107**, 043107 — Published 10 April 2023

DOI: 10.1103/PhysRevA.107.043107

The Effects of Tampering on Rare-Gas Core-Shell Clusters Irradiated by Resonantly Tuned Soft-Xray Pulses

Rishi Pandit[1], Valerie Becker[1], Jeremy Thurston[1], Kasey Barrington[1], Zachary Hartwick[1], Nicolas Bigaouette[2], Lora Ramunno[2], Edward Ackad[1]

[1]*Department of Physics, Southern Illinois University Edwardsville, Edwardsville, Illinois 62026, USA and*

[2]*Department of Physics, University of Ottawa, Ottawa, Ontario K1N 6N5, Canada*

(Dated: March 22, 2023)

Tampering resonant rare-gas clusters with non-resonant atoms has been shown to significantly decrease in the final ionization of the resonant atoms [1], but not their transient ionization [2]. In this work, we explain the details of the charge transfer mechanism from the resonant to non-resonant atoms. We have applied our model to the interaction of an ultra-intense x-ray laser tuned to the center of xenon's giant 4d resonance with core-shell argon-xenon clusters. Our results are in agreement with previous experimental results of the disintegration products [1], and the transient states [2]. Also, our model predicts that the resonant xenon is quickly ionized by the laser. The freed electrons then collisionally ionized the outer argon atoms before recombining with the inner xenon ions to reduce their final charge state. We find that unlike homogeneous clusters whose behavior is governed by the number of atoms, the behavior of core-shell heterogeneous clusters is well predicted by the ratio of resonant to non-resonant atoms.

I. INTRODUCTION

The behavior of dense matter under intense laser irradiation has been studied for decades in order to understand the basic dynamics of plasmas. In the near-infrared regime, the plasma dynamics are primarily governed by the collective behavior of delocalized electrons and are thus significantly driven by the laser. Shorter wavelength regimes, such as the extreme ultraviolet (XUV) and beyond, behave differently since the laser communicates directly with atomic electrons and is thus sensitive to the internal energy levels of the

atomic system which is element specific. This communication takes the form of ionization and/or excitation of the atomic electrons. The x-ray regime offers new insights since one or more of the internal energy levels can have resonant transitions with the laser, allowing for the study of very intense and short-duration energy absorption by the target and resulting in different subsequent behavior compared with non-resonant targets. Clusters are often used as targets in intense laser-matter interaction studies since they bridge the gap between gas and solid phases of matter with almost solid density, but no bulk for energy to easily dissipate through. Additionally, the cluster's size sets the boundary for the plasma and thus has a strong influence on the absorption of energy from the laser [3] and how the plasma evolves [4].

Over the last decade heterogeneous, layered, rare-gas clusters have been used experimentally as the target for resonant/non-resonant nanoplasma interaction studies, giving insight into how dense nanoplasmas interact [1, 2, 5]. Heterogeneous clusters are a core cluster of one rare-gas covered by layers of a different rare-gas. When irradiated, the two-element ion-plasma can behave very differently from homogeneous clusters. This difference can be enhanced by choosing the inner cluster's element to have resonant transitions with the x-ray laser. Hoener et al. [1] first measured the disintegration products of xenon gas, pure argon clusters, pure xenon clusters, mixed argon and xenon clusters, and layered xenon-argon clusters when irradiated with intense $\lambda = 13.7$ nm x-rays, which is at the center of xenon's so-called giant 4d resonance that has a full-width-at-half-maximum of about 40 eV in the cross-section [6]. They found that very high charge states of xenon (Xe^{9+}) were detected in all cases of pure xenon (gas or clusters). However, heterogeneous clusters of xenon showed no clear ion signal beyond Xe^{2+}. Further insight into the transient state of the nanoplasmas was recently obtained using XUV-spectroscopy which allows for the determination of transient charge states which have lifetimes on the femtosecond timescale [2]. Among their results, Schroedter et al. showed that the spectra from the heterogeneous clusters contained very high transient charge states as high as those detected in xenon gas and pure-xenon clusters as disintegration products. This was clear experimental evidence that the resonant xenon was ionizing to very high charge states in the heterogeneous clusters as it had in gas and homogeneous clusters, but it was undergoing significant recombination prior to disintegration. The details of the mechanism(s) behind the significant recombination of the xenon ions was unclear and is explored in this work.

Further interest in heterogeneous clusters is as a model system for the embedding of biomolecules to delay the expansion prior to imaging [1, 7]. By coating the outer layer of a biomolecule with a non-resonant, non-reacting, weakly scattering, element such as argon, ionization damage to the biomolecule can be slowed for a short while. It is hoped that this can improve the time that x-ray diffraction imaging pulses have to create an image before significant disintegration of the biomolecule occurs. Recombination as the source of the reduced charge states in as a function of the number of layers was examined by Ziaja et al. [8] outside of xenon's resonance. They examined the role recombination played in changing the atom-to-ion fraction of the cluster by running simulations with and without recombination for different numbers of layers and when the elements of the tampering layer were switched with the core element. This work was in the XUV, away from xenon's giant resonance and at an intensity much lower than the experiments, but addressed the general role of recombination in heterogeneous clusters far below their saturation intensity (when a cluster can no longer be ionized by the laser, c.f. [9]).

In the present work, we extend our atomistic classical/quantum hybrid-model of laser-cluster interaction in the XUV to reproduce the results of the heterogeneous experiments [1, 2] and then use our simulations to understand the details of the interaction. Insights into the transient state of the system are given and then generalized to the behavior of all layered heterogeneous clusters irradiated at or beyond their saturation intensity.

II. METHODS

We solve for the motion of all the particles using molecular dynamics, initially with a neutral cluster in a relaxed configuration. Initial positions of the atoms are determined by molecular dynamics with only the Van der Waals potential between the atoms. Subsequently, the relaxed cluster is irradiated with the x-ray pulse where the following mechanisms are accounted for: single-photon and multiphoton outer shell ionization, inner shell ionization, and inverse Bremsstrahlung heating (IBH). Inner ionization is followed by Auger decay as described in reference [10] and allow for the ionization of an inner electron (from the 4d shell which is resonant to ionization around 13 nm) followed later by the autoionization of valence electrons (Auger electrons). Additionally, the freed electrons may ionize or excite atoms or ions [11]. Excited electrons may then be subsequently ionized via a collision

with a free electron. Lastly, many-body recombination is also included as described in reference [10]. Many-Body recombination (MBR) from ref. [12] is therefore included in the XUV by a recombination of an electron to the ground state of the ion, followed by a collisional excitation or an ionization via single-photon ionization or direct collisional ionization. Ionization is performed using experimental (when available) or theoretically calculated cross-sections from gas. The influence of the cluster's potential on the ionization process is approximated as constant and removed for the ionization event using the Local Ionization Threshold (LIT) model, which has been shown to be well justified [13] and able to reproduce experimental signals [4].

The following parameters were used for the simulations: a constant timestep of 0.75 attoseconds, a well-depth of 0.9 Hartree, an electron recombination range of 0.1 nm, and initial simulation time of 1500 femtoseconds. This is followed by a second step calculation for at least 2 ps with recombination and no ionization until the time-of-flight field is the dominant force on the particles. That initiates the third stage in which the arrival time at the detector is calculated using the final velocity of the second step by solving the equations of motion. All these parameters have been tested and give convergent results, i.e. changing any of these to more accurate but time-consuming values, such as a smaller timestep, does not change any of the results by a meaningful amount.

Previous work with the low intensity regions of the pulse, by our group, indicated that in a heterogeneous cluster direct ion-atom charge transfer could play a role [10]. At low intensities, it becomes probable that an ion will collide with an atom. The few ionized ions repel each other and begin moving away from the cluster. They can then collide with the neutral atoms which remain stationary on their way out of the cluster's core. In the case of heterogeneous clusters, this transfer is noticeable. In the regime of the giant xenon resonance, even low intensity pulses cause significant ionization to the xenon atoms while leaving the argon atoms virtually untouched. However, since xenon is in the core of the cluster, xenon ions exiting the cluster can transfer some or all of their charge (by capturing an argon atom's electrons). Thus, the charge transfer between xenon and argon was included in this work using the experimental cross-sections of Refs. [14–16].

Time-of-flight (TOF) signals were created following the methodology outlined in reference [10]. Single cluster sizes were used, $N = 55, 147, 309, 561, 923$, at different intensities

with a 2σ cutoff $\left(I = I_0 e^{-\frac{(2\sigma)^2}{2\sigma^2}}\right)$ of the lowest intensities from the peak intensity to mimic the experimental conditions [17] of removing the spatial wings of the pulse. The core of all the clusters in this work was pure xenon, with the outer icosahedral shell(s) being argon. Only complete shells of each element were used.

III. RESULTS

Xenon core clusters with argon outer shells were exposed to similar conditions as in the experiment [1], with $I = 2.5 \times 10^{14}$ W/cm^2, $\lambda = 13.7$ nm and a full-width-at-half-maximum of 10 fs. The ionization of the cluster primarily proceeds via photoionization of the xenon atoms -mostly through inner d-shell ionization- due to the laser's wavelength being tuned to the center of the xenon giant resonance. The cross-section for xenon at 13.7 nm is 24.7 Mbarns while argon is only 1.4 Mbarns [1]. However, while the initial ionization of the cluster is straightforward, the charge state dynamics during the disintegration are not. In the following, we present our comparison to the experimental time-of-flight (TOF) signal, our comparison to the transient states detected via fluorescence imaging, and explore the effect of the composition of the cluster on its dynamics.

A. Final States

One of the most striking features of Hoener et al.'s [1] xenon-argon layered heterogeneous time-of-flight (TOF) results is the missing xenon high charge-state peaks. Between the Ar^{1+} and Ar^{2+} peaks there are no xenon peaks. Peaks up to Xe^{9+} were found in both the gas and xenon cluster TOF signals. Thus, any model must have the charge states above at least Xe^{3+} decrease to negligible amounts due to the outer layer of argon in order to match the experimental signal. Thus, a key indicator that any laser-cluster model is representing the charge transfer between the elements accurately is the lack of a significant Xe^{4+} and Xe^{5+} signal.

The detection of Xe^{3+} was unclear in the experimental time-of-flight signal, which measures the mass to charge ratio due to xenon being almost three times more massive than argon. Thus, the Xe^{3+} peak appears in the same location as the Ar^{1+} peak which may have obscured its detection.

The TOFs of Xe_{147} clusters were calculated with either one ($N_{Ar} = 162$, $N_{total} = 309$ solid dark blue for xenon, dashed dark red for argon) or two ($N_{Ar} = 414$, $N_{total} = 561$ sold light blue for xenon, dashed light red for argon) atom(s) thick layers of argon and shown in figure 1. The single-layered cluster has significantly higher charged states for both xenon and argon compared with the two-layered, despite being a smaller cluster overall ($N = 309$). The additional argon layer reduces the amount of final ionization (at the detector) resulting in almost no $Xe^{>3+}$ peaks. The most significant difference between the experimental signal and figure 1's is the lack of dimers and the relative size of the Xe^{1+} signal for both singly and doubly-layered clusters. The relative size of the Xe^{1+} signal and the lack of dimers are likely due to our model only considering pristine clusters (no fragmented or incomplete clusters).

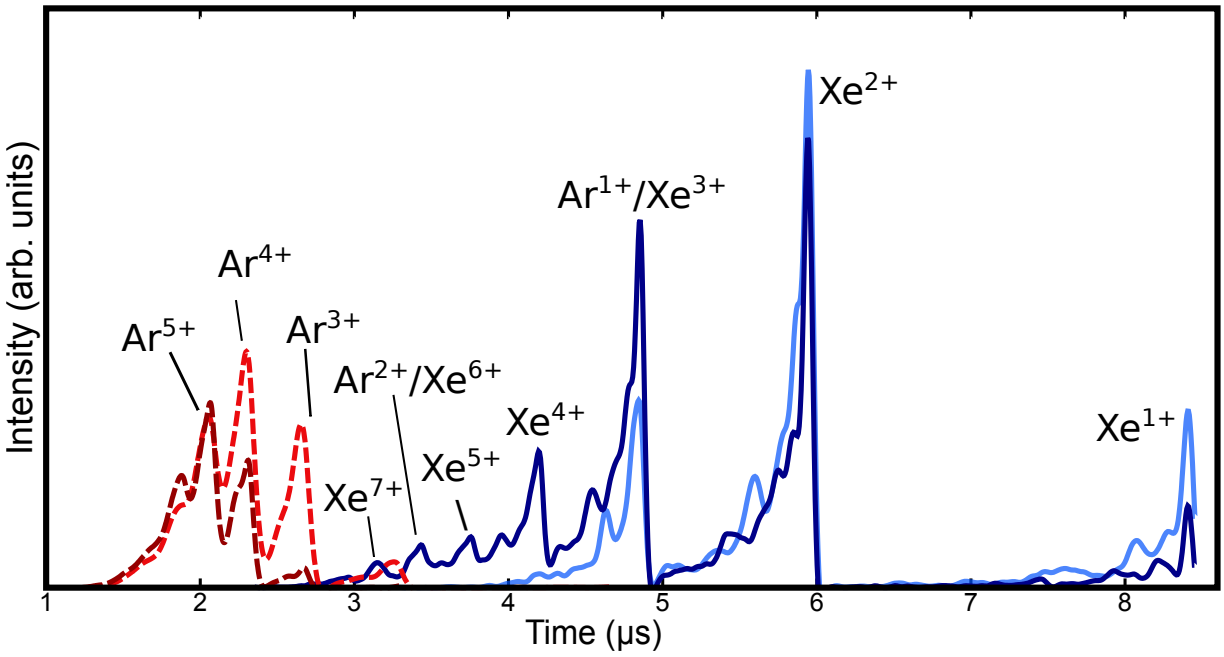

FIG. 1. The calculated time-of-flight signal for single-layered core-shell ($N_{Xe} = 147$, $N_{Ar} = 162$) heterogeneous clusters shown as the solid dark blue lines for xenon and dashed dark red lines for argon along with the two-layered core-shell ($N_{Xe} = 147$, $N_{Ar} = 414$) heterogeneous clusters shown as light blue solid lines for xenon and light red dashed lines for argon.

Two layers of argon sufficiently damp the Xe^{4+} and Xe^{5+} peaks. This provides the closest match to the experimental signal for clusters estimated to have a total size of $\langle N \rangle = 400$ with an estimated $\Delta N \approx N$ [1]. The heterogeneous cluster with a single layer of argon deviates significantly from the experimental signal and was most likely only a small proportion of the

cluster beam. It is likely that smaller clusters were present and our data suggests that they had more than a single outer-layer of argon.

The disagreement in the higher charge states of argon ($Ar^{>4+}$) is possibly due to the presence of O^{2+} in the experimental signal. However, the trend is clear: despite the two-layered argon cluster being larger than the single layered cluster, significantly less ionization occurs.

An analysis of our simulations has shown that direct charge transfer ($Xe^{q+} + Ar \rightarrow Xe + Ar^{q+}$) is found to play a negligible role. For these heterogeneous systems with a resonant core, our data does not support the model of charge transfer where the xenon is ionized and collides with the argon atoms and *directly* transfers their charge to the argon. We find that high intensity and ultrashort pulse duration result in nearly every atom being ionized via direct photoionization or collisional ionization very quickly (not shown). The photoionization-resonant xenon atoms are ionized earlier (100% xenon ions by 8 fs at $I = 2 \times 10^{13}$ W/cm^2) than the argon ions due to the direct nature of the ionization mechanism: photoionization vs collisional ionization. Nevertheless, the argon atoms become completely ionized prior to the xenon ions reaching the proximity needed for direct ion-atom charge transfer. The ion-ion repulsion is larger than the center-of-mass energy of the argon-xenon system. The end result is that only a negligible amount of ion-atom collisions occur at intensities above 10^{13} W/cm^2. Indeed, the clusters in the experiment are not exposed to those lower intensities due to the 2σ cutoff of the laser pulse performed in the experiment; thus even though we integrate over the pulse's spatial profile, these low intensities are not included.

B. Transient States

Further modeling was done using the experimental conditions of reference [2, 5] in which fluorescence imaging was used to determine the transient charge states in the cluster. The pulse parameters were $I = 2 \times 10^{15}$ W/cm^2, $\lambda = 13.5$ nm, and a much longer full-width-at-half-maximum of 150 fs. The experimental fluorescence signal found clear evidence of charge states as high as Ar^{7+} and $Xe^{>9+}$ for clusters of similar size and composition as Hoener et al. with $\langle N \rangle = 480$.

Our model's results are in qualitative agreement with these maximum charge states for clusters of $Xe_{55}Ar_{254}$ (see figures 2 and 3). Other sized clusters were also investigated,

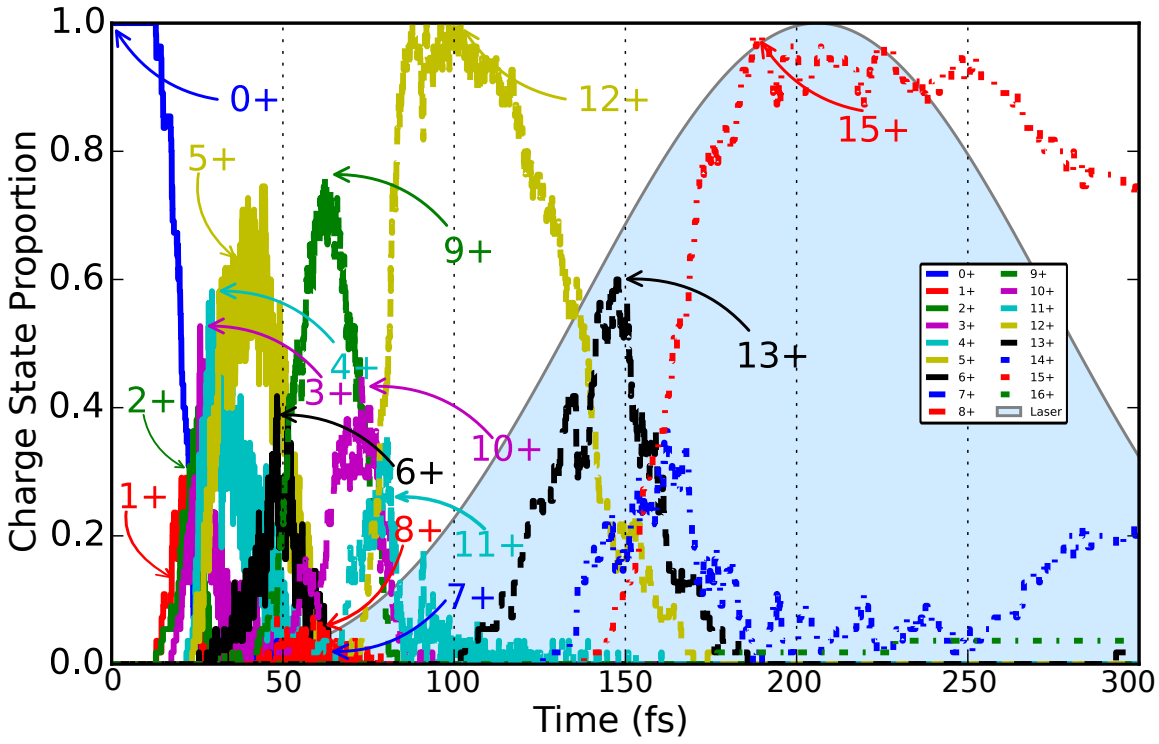

FIG. 2. The xenon charge state distribution as a function of time for a core-shell $Xe_{55}Ar_{254}$ cluster at the peak of a $I = 2 \times 10^{15}$ W/cm^2, $\lambda = 13.5$ nm and with a full-width-at-half-maximum pulse duration of 150 fs pulse.

$Xe_{55}Ar_{506}$ and $Xe_{147}Ar_{414}$ (not shown), as well as homogeneous xenon clusters Xe_{55}; all were found to give very similar results due to the clusters being saturated [9], i.e. unable to photoionize due to a lack of targets. Our model predicts that there is a segment of time (around 100 fs) before the peak of the pulse when almost the entire xenon population reaches a charge state of Xe^{12+}, and a later time (around 200 fs), near the peak of the laser pulse, when more than 90% of the xenon population is Xe^{15+}.

The argon population saturates more quickly than the xenon population, achieving stable charge state ratios by around 100 fs (figure 3). The population at this time consists of about 80% Ar^{5+} and almost 20% Ar^{6+}. This is in contrast to a solid, homogeneous, argon cluster of sizes $Ar_{55/147/309}$ which only saturate at around 250 fs (for the same laser pulse) to nearly 100% Ar^{5+} (not shown). Thus, the xenon inner-core significantly increases the rate and overall ionization of the non-resonant argon.

The discrepancy between our results and the experimental signal primarily lay with the

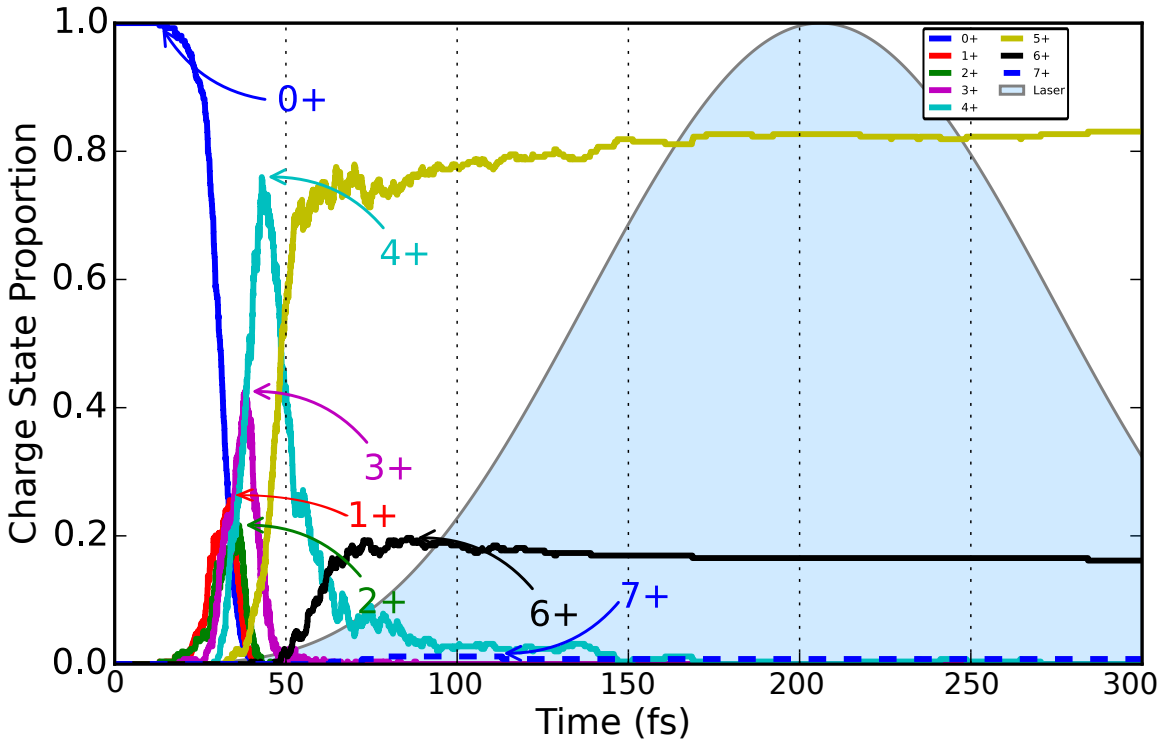

FIG. 3. The argon charge state distribution as a function of time for a core-shell $Xe_{55}Ar_{254}$ cluster at the peak of a $I = 2 \times 10^{15}$ W/cm^2, $\lambda = 13.5$ nm and with a full-width-at-half-maximum pulse duration of 150 fs pulse.

small population of Ar^{7+} at around 100 fs. The fluorescence spectra found a large (nearly 20%) increase in the abundance of Ar^{6+} and Ar^{7+} in xenon-core-argon-shell clusters compared with pure argon clusters [2]. We would, thus, expect that our model should have roughly equal populations of these high charge states and some Ar^{8+} which would fluorescence as Ar^{7+}. However, we only see a small population of Ar^{7+} and no Ar^{8+} (c.f. Fig. 3). This suggests that the model may not be capturing all the excitation and ionization. However, this seems specific to the argon population as the xenon population does see an abundance of charge states capable of generating the fluorescence signals detected. One likely possibility is that the additional argon fluorescence (Ar^{7+} in the experimental spectra) is driven by photoexcitation of the Ar^{6+} $2p^6 3s^2\ ^1S_0$ to $3s5p\ ^1P_1$ (at 13.4797 nm) which is not included in our model [18]. This would excite much of the Ar^{6+} population and be quickly followed up by collisional ionization from the excited state. This would drive the Ar^{6+} population to become Ar^{7+} which could then further ionize to Ar^{8+}, or be excited to a

state which can then fluorescence (creating the additional Ar^{+7} signal). Another would be that the cluster size or composition in our model differs from the experiment.

C. The effect of cluster composition

Our results from one and two-layered heterogeneous clusters, shown in Fig. 1, disagree with the general trend that the amount of ionization is proportional to the size of the cluster [4, 19]. Further investigations were undertaken to assess what the general trends are that drive the dynamics of the heterogeneous system. Our initial investigations attempted to link the dynamics of the cluster to the number of layers (from one to four layers) and were only marginally successful (not shown). However, relating our calculated dynamics of the heterogeneous cluster to the argon-to-xenon number ratio, ρ, was found to be much more accurate. We show below that the behavior and signals from a heterogeneous cluster are a function of the argon-to-xenon number ratio through a broad range of cluster sizes, just as the number of atoms in a cluster predicted the behavior and signals of a homogeneous cluster [4, 19]. Moreover, no other parameter (cluster size, N_{Xe}, N_{Ar}, number of layers) could accurately predict the behavior and calculated signals of the heterogeneous clusters.

There are three different average ion charge states (AICS) in a two-element heterogeneous cluster: the xenon average ion charge state, the argon average ion charge state and the total average ion charge state; note that atoms are not included in the averages. All three cases are shown, for the disintegration products of a cluster at the peak of the laser pulse, as a function of the argon-to-xenon number ratio in figure 4 for similar conditions as references [2, 5], with $I = 2 \times 10^{15}$ W/cm^2, $\lambda = 13.5$ nm and a full-width-at-half-maximum of 150 fs. Each AICS is separately fitted and the results are plotted in figure 4 (a solid black line for the total AICS, a dotted green line for the xenon AICS, and dashed blue line for the argon AICS), by the empirical model

$$AICS(\rho) = C + \frac{A}{\rho^n + B}, \tag{1}$$

where ρ is the argon-to-xenon number ratio, C is a fitting parameter that gives the AICS for infinitely tampered samples ($\rho \to \infty$ or an infinite number of argon layers), and A, B, and n are the other fitting parameters. Good agreement for C is found with the above empirical model and our simulations of pure argon clusters, which are in a state of induced transparency at these intensities (see reference [9]).

As expected, the argon AICS is the lowest and the xenon AICS is highest when the ratio is less than 1 (more xenon than argon). With a ratio above 1, the argon has a higher AICS than the (resonant) xenon. This is the hallmark of the xenon-to-argon charge transfer.

The larger the proportion of argon, the lower the three AICSs are. The replacement of a resonant xenon atom with a non-resonant argon atom explains this result for small ratios ($\rho < 3$). By exchanging a high ionization cross-section xenon atom with a low cross-section argon atom the amount of energy absorbed by the cluster is reduced. However, this decrease due to the lower cross-section of the argon changes from almost linear when $\rho < 3$ to being almost constant when $\rho > 6$. This suggests there is a threshold in the behavior of the cluster near $\rho \approx 4$, which is due to a cascade ionization process. The cascade is initiated by the photoionization of the resonant xenon population, and it grows as the freed electrons collisionally ionize other electrons. The larger slope of the xenon AICS indicates that the cascade primarily ionizes the xenon population. It is important to note that because inverse Bremsstrahlung heating (IBH) is negligible in this regime, the cascade is only driven by the laser *pre*-ionization, and not *post*-ionization. Thus, all the energy imbued into the electron plasma by the laser is due to the excess energy of the photon above the ionization potential and no significant amount of energy comes from the laser's field (though IBH) as is the case for longer wavelengths [9].

Many different sized clusters are represented in figure 4. The inset in figure 4 again shows the total AICS as a function of the argon-to-xenon number ratio, but with the total size of the cluster shown as different symbols. Clusters as small as $N = 309$, to as large as $N = 5083$ are represented and fall along the geometric fit. The success of the fit through more than an order of magnitude in cluster size suggests the behavior of heterogeneous clusters is governed by the xenon-to-argon ratio in the same way cluster size governs the behavior of homogeneous clusters [4, 20].

IV. CONCLUSION

The effects of tampering a resonant cluster with a non-resonant material have been explored using a resonant xenon-core tampered with an outer layer of argon. The results of our model explain the charge transfer in Hoener et al. [1] to be due to ion-electron recombination without any direct charge transfer between the ions. The fluorescence signals

from Schroedter et al. [2] qualitatively match our model's transient state predictions and show how the cluster's photoionization becomes saturated in the outer, non-resonant layer. The core continues to ionize primarily due to collisional ionization being highly effective due to the higher density in the core of the cluster. This two-atomic species interaction allows for the resonant atoms to become highly ionized, but maintain their relative position. Additionally, these ions transfer much of their ionization through the electron plasma to the non-resonant species. Lastly, a new general trend is that the resonant-to-non-resonant ratio is what determines the behavior of the heterogeneous cluster, not simply the cluster size as is the case with homogeneous clusters.

V. ACKNOWLEDGMENTS

This work was supported by the Air Force Office of Scientific Research under AFOSR Award No. FA9550-14-1-0247. Some of this work used the XStream computational resource, supported by the National Science Foundation Major Research Instrumentation program (ACI-1429830) with improved infrastructure access supported by the National Science Foundation Networking Infrastructure award (1541435). V. B. was partially supported by the Blue Waters Student Internship Program, part of the Blue Waters sustained-petascale computing project, which is supported by the National Science Foundation (awards OCI-0725070 and ACI-1238993) and the state of Illinois. Blue Waters is a joint effort of the University of Illinois at Urbana-Campaign and its National Center for Supercomputing Applications.

---

[1] M. Hoener, C. Bostedt, H Thomas, L. Landt, E. Eremina, H. Wabnitz, T. Laarmann, R. Treusch, a R. B. De Castro, and T. Möller. Charge recombination in soft x-ray laser produced nanoplasmas. *Journal of Physics B: Atomic, Molecular and Optical Physics*, 41(18):181001, September 2008.

[2] L. Schroedter, M. Müller, A. Kickermann, A. Przystawik, S. Toleikis, M. Adolph, L. Flückiger, T. Gorkhover, L. Nösel, M. Krikunova, T. Oelze, Y. Ovcharenko, D. Rupp, M. Sauppe, D. Wolter, S. Schorb, C. Bostedt, T. Möller, and T. Laarmann. Hidden Charge States in Soft-X-Ray Laser-Produced Nanoplasmas Revealed by Fluorescence Spectroscopy. *Physical Review Letters*, 112(18):183401, May 2014.

[3] J. Zweiback, T. Ditmire, and M.D Perry. Resonance in scattering and absorption from large noble gas clusters. *Opt. Express*, 6(12):236–242, Jun 2000.

[4] Edward Ackad, Nicolas Bigaouette, Kyle Briggs, and Lora Ramunno. Clusters in intense xuv pulses: effects of cluster size on expansion dynamics and ionization. *Phys. Rev. A*, 83:063201, Jun 2011.

[5] A. Przystawik, L. Schroedter, M. Müller, M. Adolph, C. Bostedt, L. Flückiger, T. Gorkhover, A. Kickermann, M. Krikunova, L. Nösel, T. Oelze, Y. Ovcharenko, D. Rupp, M. Sauppe, S. Schorb, S. Usenko, T. Möller, and T. Laarmann. Ionization dynamics of Xe nanoplasma formation studied with XUV fluorescence spectroscopy. *Journal of Physics B: Atomic, Molecular and Optical Physics*, 48(18):184002, sep 2015.

[6] P. Andersen, T. Andersen, F. Folkmann, V.K. Ivanov, H. Kjeldsen, and J.B. West. Absolute cross sections for the photoionization of 4d electrons in Xe+ and Xe2+ ions. *Journal of Physics B: Atomic, Molecular and Optical Physics*, 34(01):2009, 2001.

[7] Stefan P. Hau-Riege, Richard A. London, Henry N. Chapman, Abraham Szoke, and Nicusor Timneanu. Encapsulation and diffraction-pattern-correction methods to reduce the effect of damage in x-ray diffraction imaging of single biological molecules. *Phys. Rev. Lett.*, 98:198302, May 2007.

[8] B. Ziaja, H. N. Chapman, R. Santra, T. Laarmann, E. Weckert, C. Bostedt, and T. Möller. Heterogeneous clusters as a model system for the study of ionization dynamics within tampered samples. *Physical Review A*, 84(3):033201, September 2011.

[9] R. Pandit, K. Barrington, T. Teague, V. Becker, J. Thurston, Z. Hartwick, N. Bigaouette, L. Ramunno and E. Ackad. Induced transparency in the XUV: a pump-probe test of laser-cluster interactions. *J. Phys. Commun.*, 2018.

[10] Edward Ackad, Nicolas Bigaouette, Stephanie Mack, Konstatin Popov, and Lora Ramunno. Recombination effects in soft-x-ray cluster interactions at the xenon giant resonance. *New Journal of Physics*, 15(5):053047, 2013.

[11] Edward Ackad, Nicolas Bigaouette, and Lora Ramunno. Augmented collisional ionization via excited states in xuv cluster interaction. *J. Phys. B*, 44:165102, 2011.

[12] Christian Jungreuthmayer, Lora Ramunno, Jurgen Zanghellini, and Thomas Brabec. Intense vuv laser cluster interaction in the strong coupling regime. *J. Phys. B*, 38(16):3029–3036, 2005.

[13] Jeff White and Edward Ackad. A validation of a simple model for the calculation of the ionization energies in x-ray laser-cluster interactions. *Physics of Plasmas*, 22(2):022123, 2015.

[14] T. Kusakabe, T. Horiuchi, N. Nagai, H. Hanaki, I. Konomi, and M. Sakisaka. Charge transfer of multiply charged slow argon, krypton and xenon ions on atomic and molecular targets. Single-charge transfer cross sections. *Journal of Physics B: Atomic and Molecular Physics*, 19(14):2165–2174, jul 1986.

[15] N. Selberg, C. Biedermann, and H. Cederquist. Semiempirical scaling laws for electron capture at low energies. *Physical Review A*, 54(5):4127–4135, 1996.

[16] N. Selberg, C. Biedermann, and H. Cederquist. Absolute charge-exchange cross sections for the interaction between slow Xe^{q+} $(15 \leq q \leq 43)$ projectiles and neutral He , Ar , and Xe. 56(6), 1997.

[17] T. Laarmann. private communication.

[18] A. Kramida, Yu. Ralchenko, J. Reader, and and NIST ASD Team. NIST Atomic Spectra Database (ver. 5.5.6), [Online]. Available: `https://physics.nist.gov/asd` [2018, August 31]. National Institute of Standards and Technology, Gaithersburg, MD., 2018.

[19] Th. Fennel, K.-H. Meiwes-Broer, J. Tiggesbäumker, P. M. Dinh, and E. Suraud. Laser-driven nonlinear cluster dynamics. *Reviews of Modern Physics*, 82(2):1793–1842, June 2010.

[20] B. Erk, K. Hoffmann, N. Kandadai, A. Helal, J. Keto, and T. Ditmire. Observation of shells in Coulomb explosions of rare-gas clusters. *Physical Review A*, 83(4):1–5, apr 2011.

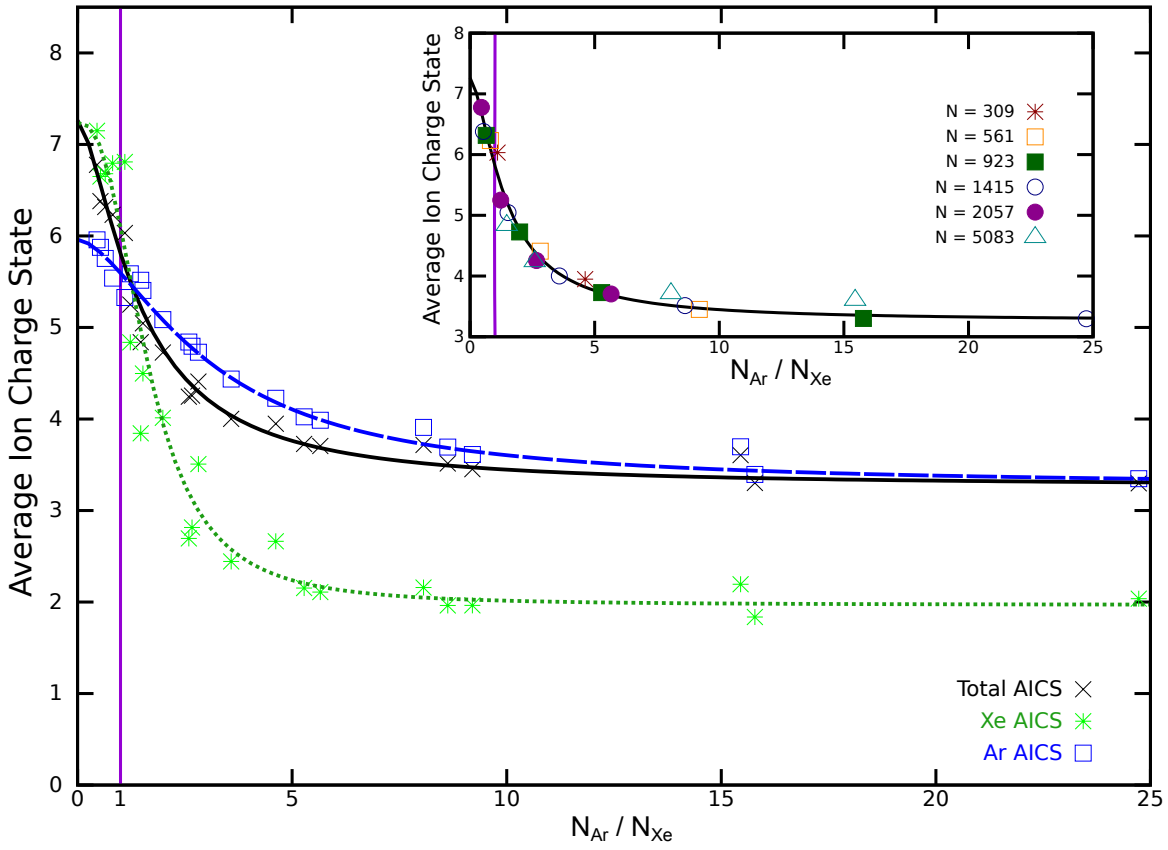

FIG. 4. The xenon (green stars), argon (blue squares), and total cluster's (black ×'s) average ion charge state (AICS) for the disintegration products of core-shell heterogeneous clusters of size $N = 309, 561, 923, 1415, 2057, 5083$ as a function of the xenon-to-argon ratio, ρ, after being irradiated by the peak of a $I = 2 \times 10^{15}$ W/cm^2, $\lambda = 13.5$ nm laser pulse with a full-width-at-half-maximum of 150 fs. A fit to the empirical model of equation 1 is shown as the dotted green line for xenon, dashed blue line for argon, and solid black line for the cluster's total AICS. The inset plots the total AICS again, but showing different symbols for the different sized clusters used. A solid vertical purple denotes $\rho = 1$, where the cluster has an equal composition of both elements.